Core-shell Hybrid Zeolitic Imidazolate Framework-derived Hierarchical Carbon for Capacitive Deionization

Wuxiang Zhang[1,2], Arramel Arramel[2], Wong Ping Kwan Johnny[3], Lei Zhang[2], Jianzhong Zheng[4], Wen Zhang[3], Hao Zhang[1], Xin Yan[1], Junwen Qi[1], Jiansheng Li [1*]

[1] Key Laboratory of Jiangsu Province for Chemical Pollution Control and Resources Reuse, Key Laboratory of New Membrane Materials, School of Environment and Biological Engineering, Nanjing University of Science and Technology, Nanjing 210094, China.

[2] Department of Physics, National University of Singapore, Singapore 117542, Singapore.

[3] School of Electronics and Information, Northwestern Polytechnical University, 127 West Youyi Road, Xi'an, Shanxi 710072, China.

[4] Department of Applied Physics, The Hong Kong Polytechnic University, Hong Kong 999077, China.

* Corresponding author: Prof. Jiansheng Li

Tel: +(86) 025-84315351 E-mail: lijsh@njust.edu.cn

Chemical materials

Zinc nitrate hexahydrate ($Zn(NO_3)_2 \cdot 6H_2O$), hydrochloric acid (HCl) and cetyl-trimethyl ammonium bromide (CTAB) were purchased from Sinopharm Chemical Reagent Co., Ltd. 2-methyimidazole (2-MI, purity 99 %) were purchased from Sigma-Aldrich. Dopamine (DA) and polyvinyl pyrrolidone (PVP) were purchased from Aladdin Industrial Corporation. Ethanol was purchased from Nanjing Chemical Reagent Co., Ltd.

Characterization

The morphology of all as-prepared samples was operated by Field-emission scanning electron microscopy (SEM) (FEI Quanta 250F system) and Transmission electron microscopy (TEM) (FEI Tecnai G20 electron microscope). The structure-property of all as-prepared samples were conducted by X-ray powder diffraction (XRD) patterns (Bruker D8 Advance, Bruker AXS, Germany), Nitrogen adsorption/desorption isotherm (Belsorp-MAX (Bel Japan, Inc.)) (The pore size distribution was estimated via the DFT models using N_2 adsorption data), X-ray photoelectron spectroscopy (XPS) (PHI Quantera II ESCA System), Raman spectra (Aramis spectrometer at 532 nm), and Thermogravimetric (TG) (SDT Q600 thermo-gravimetry/differential thermal analyzer). Electrochemistry measurements were tested in a three-electrode system by an electrochemical workstation (CHI 760D).

Electrochemistry measurements

Dispersed 10 mg of the obtained materials in 1.0 mL water and ethanol mixture solution (water: ethanol=7:3), perform the ultrasonic treatment to form the uniform ink. Then dropped the ink (5 μL) into the glassy carbon electrode with a diameter of 3 mm. After the solution was naturally dried, 2 μL of Nafion (5%) solution was dropped into the electrode. No resistance compensation is provided for all electrochemical data. Calculated specific capacitances (C, F g^{-1}) was according the CV curves by the following equation:

$$C = \int \frac{I dv}{2v \, \Delta V m} \tag{1}$$

Where C is the specific capacitance, I is the response current density, ΔV is the potential window, V is the potential scan rate and m is the mass of the electrode material.

Capacitive deionization experiment

The electrosorption property was evaluated by a self-assembly flow-through CDI device. The graphite plate with a length of 10 cm×10 cm×1 mm was used as a current collector. The as-prepared catalysts powder sample (80 % by weight), acetylene black (10 % by weight), and polytetrafluoroethylene (PTFE, 10 % by weight) were uniformly mixed in ethanol to acquire the inks. Thereafter, coating the inks into the center of the graphite plate (1 cm × 1 cm) and dried at 100 °C for 5 h. The total mass of the catalysts was 50 mg. Electrosorption experiments were carried out by a continuously circulating 30 ml of deoxygenated NaCl solution at a flow rate of 25 ml min^{-1}. Detection of changes in NaCl concentration by a conductivity meter (DDS-308, Precision & Scientific Instrument). The salt adsorption capacity (mg g^{-1}) can be calculated according to formulas as follow:

$$\Gamma = \frac{(C_0 - C_e)V}{m} \tag{2}$$

where C_0 and C_e are the initial and final salt concentrations (mg L^{-1}), V (mL) is the volume of the salt solution, and m (g) is the total mass of electrode materials.

The electrosorption rate can be measured by the Ragone diagram as shown in the following equation:

$$\Gamma_t = \frac{(C_0 - C_t)V}{m} \tag{3}$$

$$v_t = \frac{\Gamma_t}{t} \tag{4}$$

Where C_t (mg L^{-1}) means the NaCl concentration at t min, the Γ_t, (mg g^{-1}) was ECs at a certain time, and v_t, was the corresponding electrosorption rate (mg g^{-1} min^{-1}).
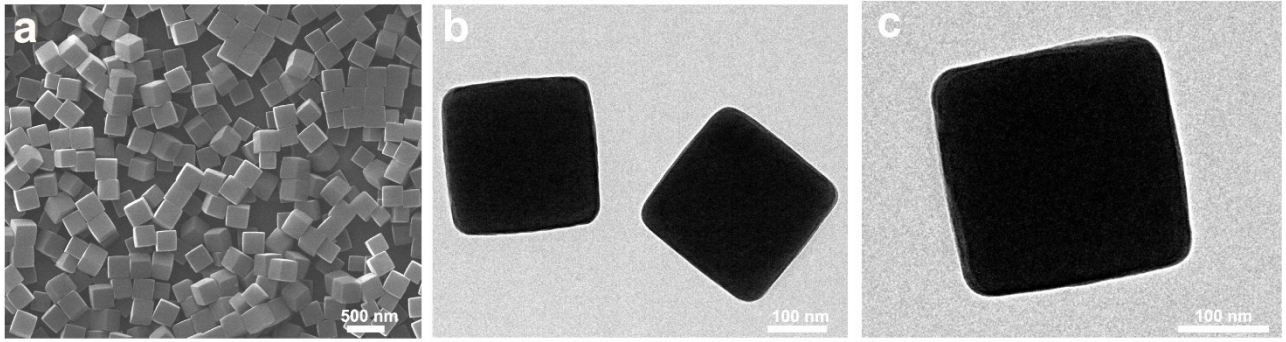
Fig.S1. (a) SEM image and (b, c) magnified TEM images of ZIF-8 particles showing a well-defined cubic shape and a uniform particle size of ~260 nm.
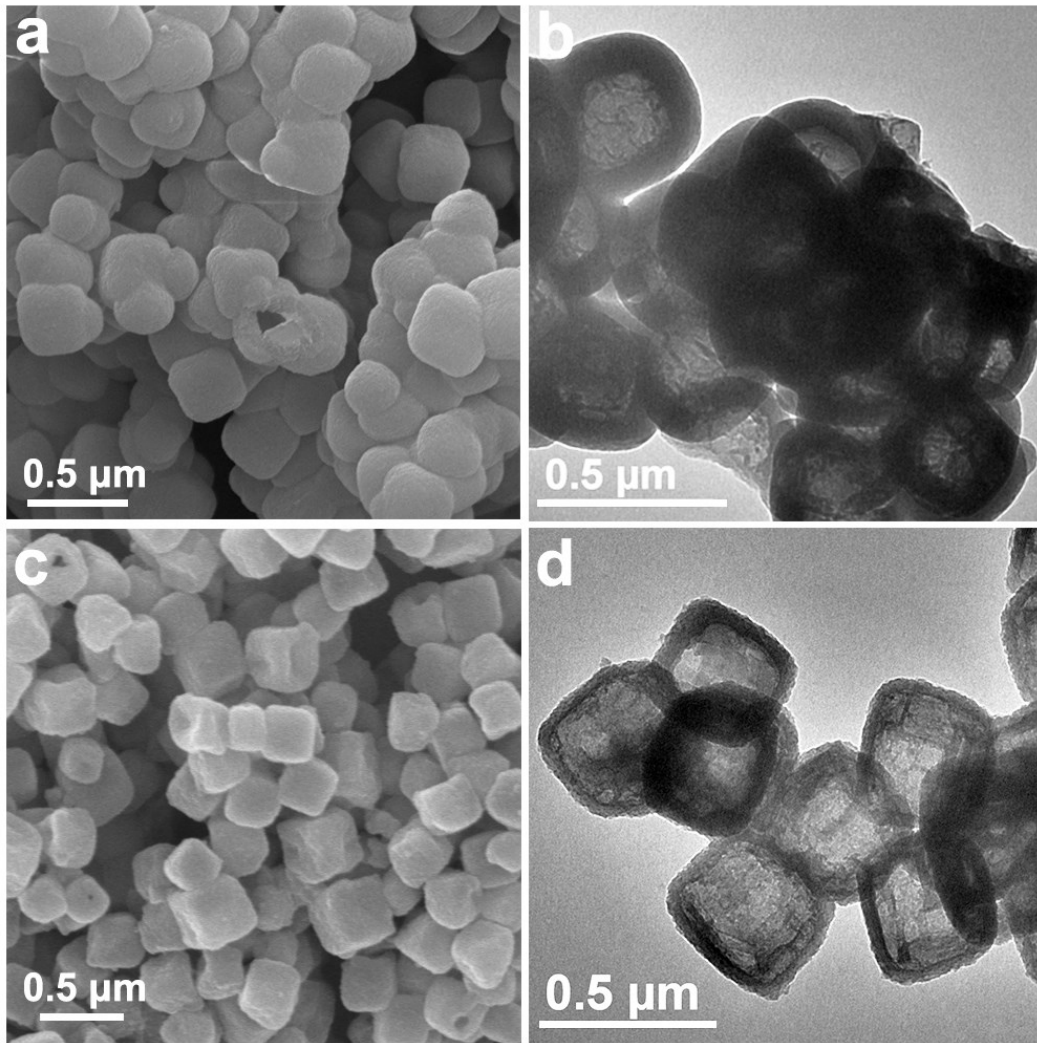
Fig. S2. (a) SEM and (b) TEM of HZIF-8/PDA-1 shows the adhesion structure with the averages particle sizes of 400 nm, TEM further shows that the aggregated particles have a large cavity with a shell thickness of 70 nm. (c) SEM and (d) TEM image of HZIF-8/PDA-2 indicates a well-dispersed and hollow cubical structure with shell thickness of 35 nm.
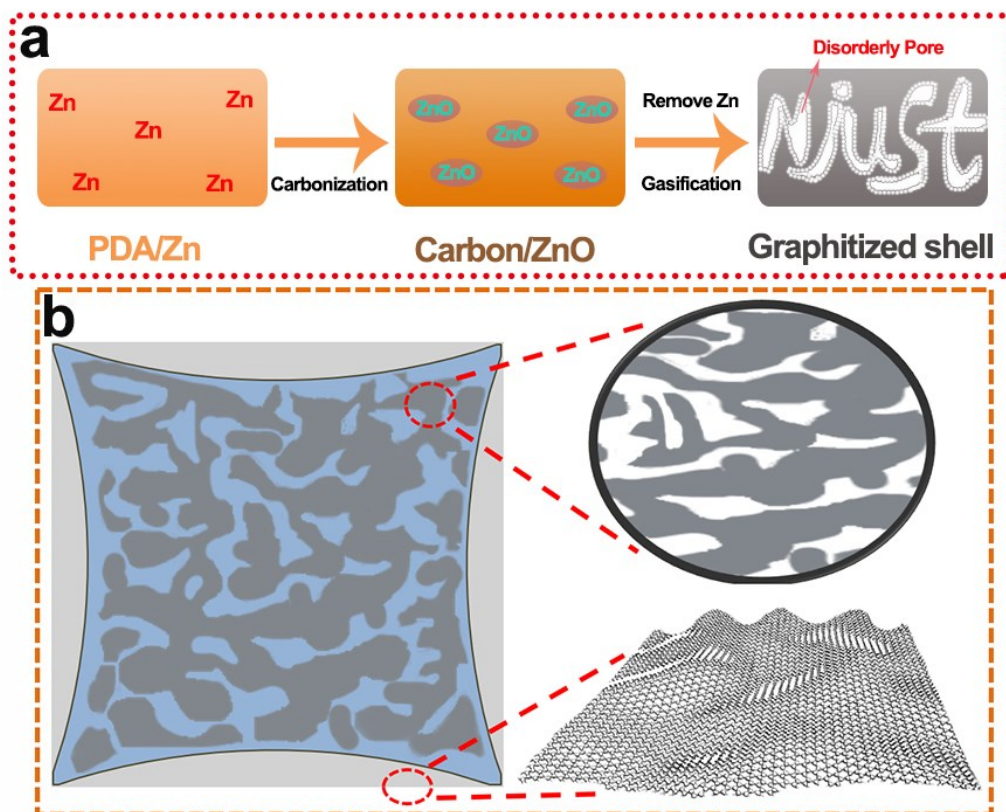
Fig. S3. (a) Schematic illustration of the porous structure formation, (b) the scheme for the structure of ANHCs nanoparticle.
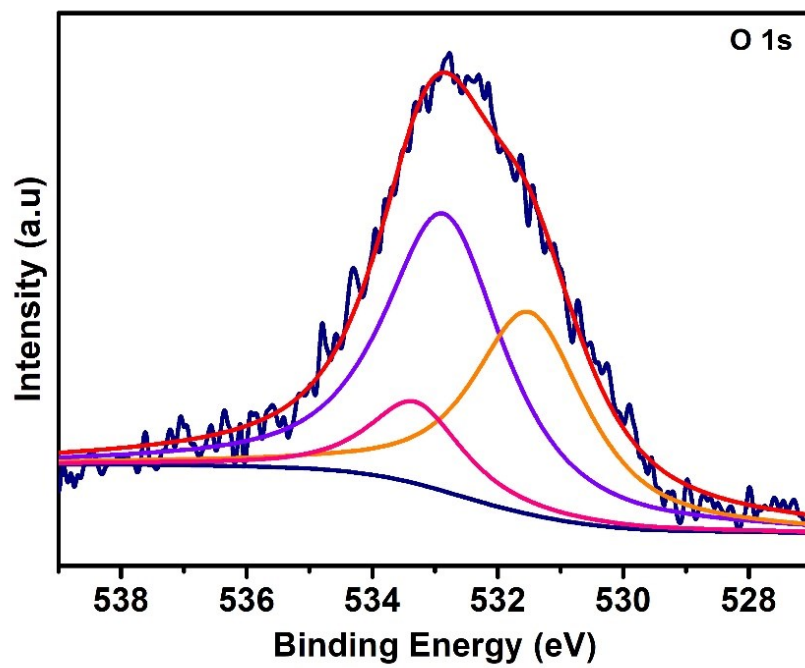
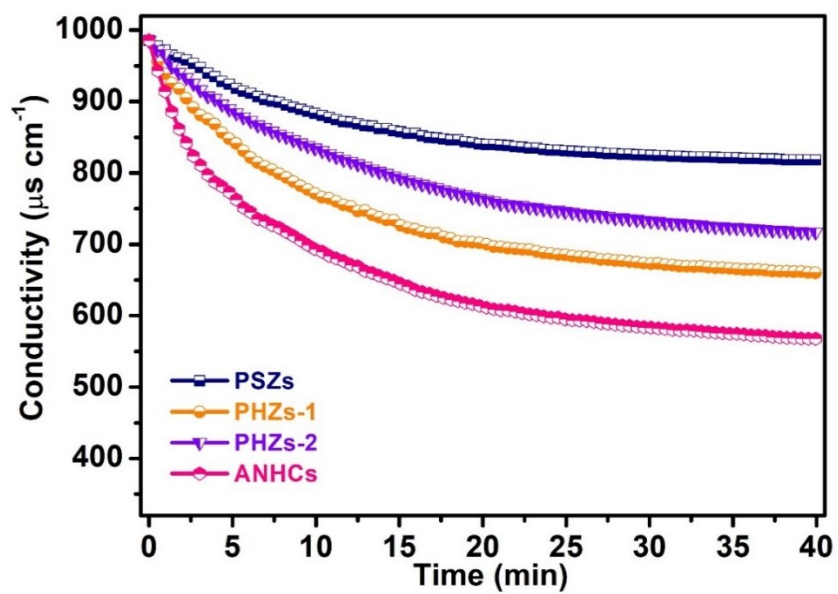Fig. S4. High-resolution O 1s XPS spectrum of ANHCs.

Fig. S5. The conductivity-time curve of PSZs, PHZs-1, PHZs-2, and ANHCs electrode.
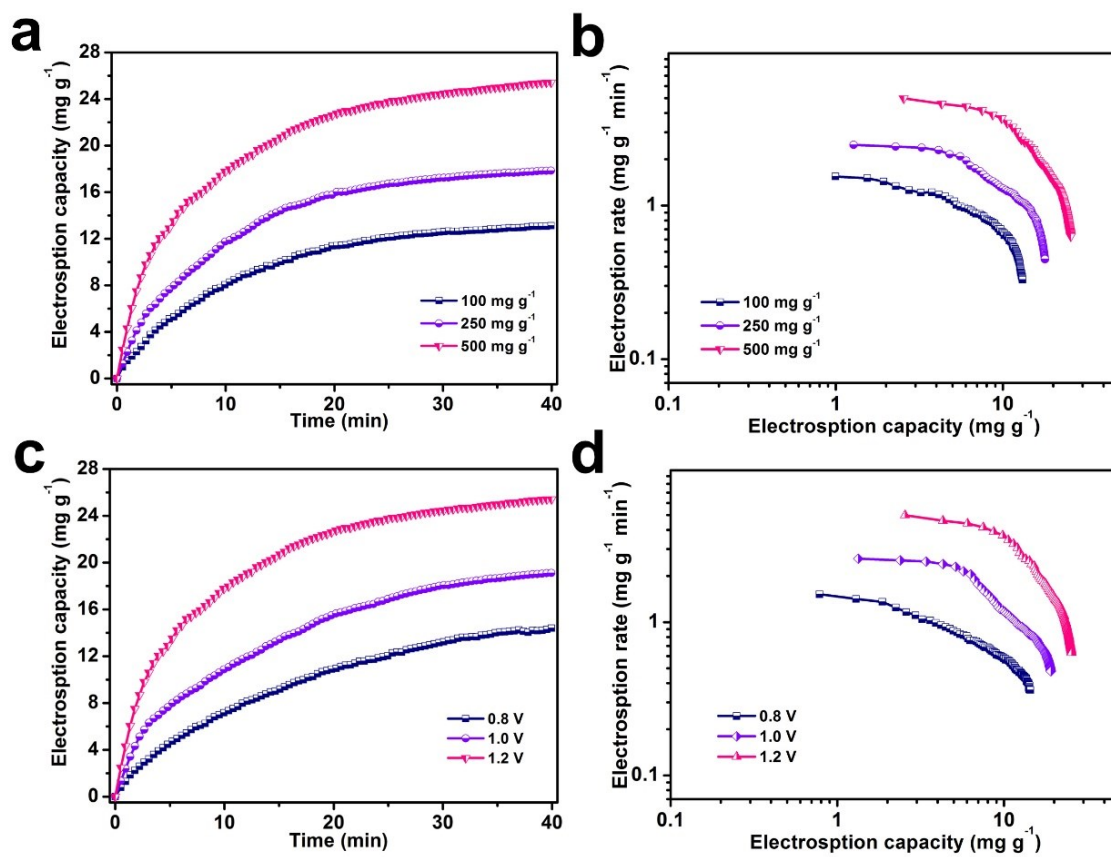
Fig. S6. (a) ECs, and (b) Ragone plots of ANHCs electrodes in 100, 250 and 500 mg g⁻¹ salt solution, (a) ECs, and (b) Ragone plots of ANHCs electrodes at 0.8, 1.0 and 1.2 V applied voltage.
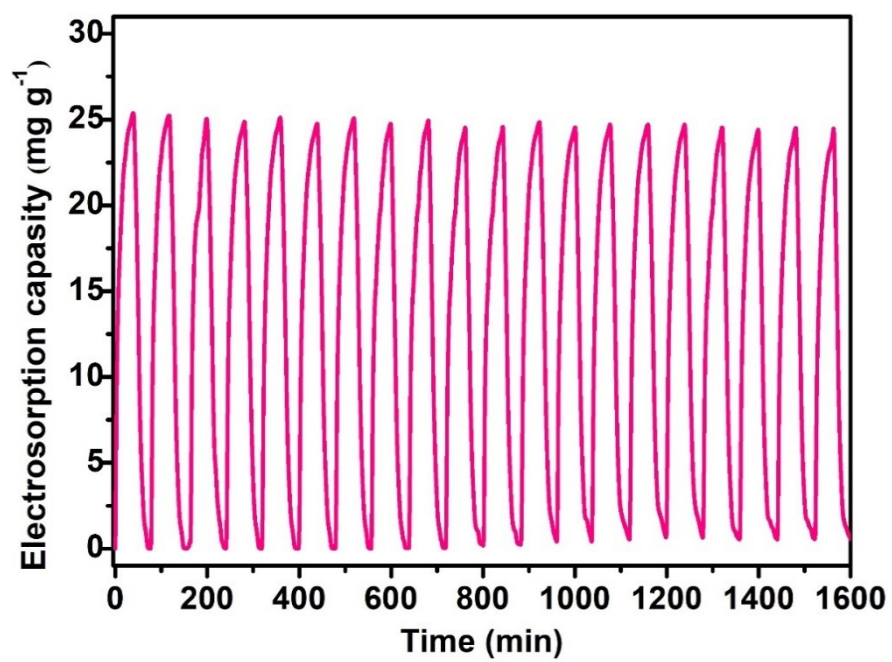
Fig. S7. Reusable experiment of ANHCs in 500 mg L^{-1} NaCl with an applied voltage of 1.2 V.
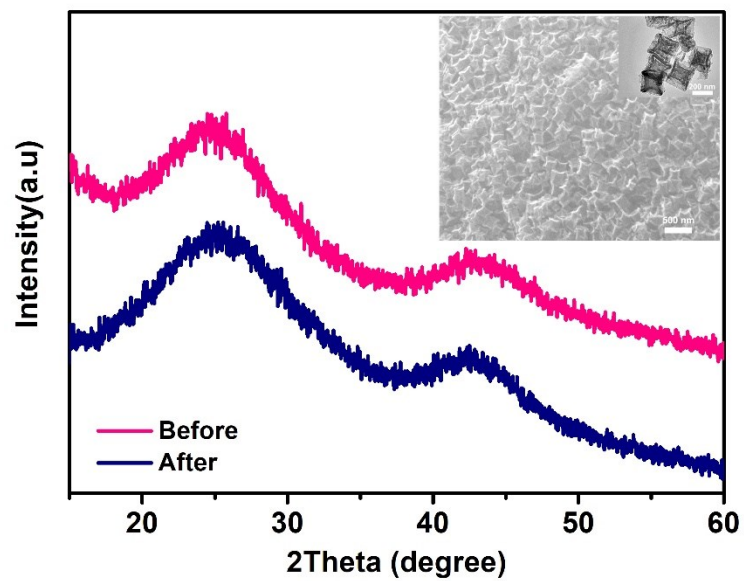
Fig. S8. XRD comparison of ANHCs before and after the cycling experiment. Inset: SEM and TEM images of ANHCs after the cycling experiment.

Table. S1. The summary element analysis of the samples.

Sample	C (%)	N (%)	O (%)
PSZs	90.41	5.14	4.45
PHZs-1	91.6	4.19	4.21
PHZs-2	90.79	2.16	7.05
ANHCs	87.29	7.12	5.59

Table. S2. typical N species analysis of the samples.

Sample	Pyridinic-N (%)	Pyrrolic-N (%)	Graphitic-N (%)	Oxided-N (%)
PSZs	24.2	20.3	39.4	16.1
PHZs-1	14.7	24.6	43.3	17.4
PHZs-2	17.4	36.2	37.3	9.1
ANHCs	26.3	21.3	42.9	9.5

Table. S3. A comparison of electrosorption capacities of recently reported carbon electrodes.

| Sample | Specific area (m^2 g^{-1}) | CDI operation conditions | | ECs (mg g^{-1}) | Ref. |
		Voltage (V)	NaCl (mg L^{-1}) Concentration		
GHMCSs	512	1.6	60.0	2.3	J. Mater. Chem. A 2014, 2, 4739.
ZIF-67/PPy	1176.8	1.2	584	11.34	Mater. Horiz. 2019, 6, 1433.
PCP	1187.8	1.2	500	13.86	Chem. Commun. 2015, 51, 12020.
SBB-CO_2-30	1019	1.2	292.5	28.9	J. Hazard. Mat., 2020, 383, 121192.
HZCs	642.7	1.6	500	19.84	Electrochim. Acta 2018, 273, 34.
ZIF-8@PZS-C	929	1.2	500	22.19	J. Mater. Chem. A 2018, 6, 15245.
A-NCP	2474	1.2	100	24.4	Chem. Eng. J., 2020, 382, 122996.
N-HCPs	512	1.4	500	12.95	Appl. Surf. Sci. 2016, 369, 460.
o-OMCs-800	750	1.2	584	14.58	Enviro. Sci-Nano, 2019, 6, 981.
N-PHCs	813	1.4	500	16.63	J. Mater. Chem. A 2016, 4, 10858.
ANHCs	872.5	1.2	500	25.4	This work